International Journal of Nanomedicine

Dovepress

open access to scientific and medical research

Open Access Full Text Article

ORIGINAL RESEARCH

Development of a Magnetically-Assisted SERS Biosensor for Rapid Bacterial Detection

Siyun Cheng[1,2,*], Zhijie Tu[2,*], Shuai Zheng[3], Adeel Khan[4], Ping Yang[1], Han Shen[1], Bing Gu[2,3]

[1]Department of Clinical Laboratory, Nanjing Drum Tower Hospital, the Affiliated Hospital of Nanjing University Medical School, Nanjing, People's Republic of China; [2]Medical Technology School of Xuzhou Medical University, Xuzhou, People's Republic of China; [3]Department of Clinical Laboratory Medicine, Guangdong Provincial People's Hospital (Guangdong Academy of Medical Sciences), Southern Medical University, Guangzhou, People's Republic of China; [4]Department of Biotechnology, University of Science and Technology, Bannu, KP, Pakistan

*These authors contributed equally to this work

Correspondence: Han Shen, Department of Clinical Laboratory, Nanjing Drum Tower Hospital, Nanjing, People's Republic of China, Tel +8602583304616, Fax +02568183912, Email shenhan@njglyy.com; Bing Gu, Department of Clinical Laboratory Medicine, Guangdong Provincial People's Hospital, Guangzhou, People's Republic of China, Tel +8602083827812, Fax +02083875881, Email gubing@gdph.org.cn

Introduction: Ultrasensitive bacterial detection methods are crucial to ensuring accurate diagnosis and effective clinical monitoring, given the significant threat bacterial infections pose to human health. The aim of this study is to develop a biosensor with capabilities for broad-spectrum bacterial detection, rapid processing, and cost-effectiveness.

Methods: A magnetically-assisted SERS biosensor was designed, employing wheat germ agglutinin (WGA) for broad-spectrum recognition and antibodies for specific capture. Gold nanostars (AuNSs) were sequentially modified with the Raman reporter molecules and WGA, creating a versatile SERS tag with high affinity for a diverse range of bacteria. *Staphylococcus aureus* (*S. aureus*) and *Pseudomonas aeruginosa* (*P. aeruginosa*) antibody-modified Fe_3O_4 magnetic gold nanoparticles (MGNPs) served as the capture probes. Target bacteria were captured by MGNPs and combined with SERS tags, forming a "sandwich" composite structure for bacterial detection.

Results: AuNSs, with a core size of 65 nm, exhibited excellent storage stability (RSD=5.6%) and demonstrated superior SERS enhancement compared to colloidal gold nanoparticles. Efficient binding of *S. aureus* and *P. aeruginosa* to MGNPs resulted in capture efficiencies of 89.13% and 85.31%, respectively. Under optimized conditions, the developed assay achieved a limit of detection (LOD) of 7 CFU/mL for *S. aureus* and 5 CFU/mL for *P. aeruginosa*. The bacterial concentration (10–10^6 CFU/mL) showed a strong linear correlation with the SERS intensity at 1331 cm^{-1}. Additionally, high recoveries (84.8% - 118.0%) and low RSD (6.21% - 11.42%) were observed in spiked human urine samples.

Conclusion: This study introduces a simple and innovative magnetically-assisted SERS biosensor for the sensitive and quantitative detection of *S. aureus* or *P. aeruginosa*, utilizing WGA and antibodies. The developed biosensor enhances the capabilities of the "sandwich" type SERS biosensor, offering a novel and effective platform for accurate and timely clinical diagnosis of bacterial infections.

Keywords: SERS, WGA, pathogenic bacteria, bacterial detection, dual-recognition

Introduction

Bacterial infections continue to pose a significant public health concern, affecting an estimated 258 million people worldwide and resulting in nearly 280,000 deaths annually.[1,2] Current methods, including plate culture,[3] polymerase chain reaction (PCR),[4] and enzyme-linked immunosorbent assays (ELISA),[5] are commonly employed for pathogen detection. These methods for bacterial detection typically take at least 48 hours to complete, involving processes such as isolation, cultivation, and identification of the bacteria. This process can be time-consuming, especially for slowly growing bacteria. Moreover, the steps involving separation and enrichment are time-consuming, potentially causing delays in achieving final and accurate bacterial detection.[6] Delays in such situations are undesirable, particularly in emergency conditions, as they pose a serious risk to patients' lives and health.

Received: 22 September 2023
Accepted: 31 December 2023
Published: 16 January 2024

Graphical Abstract

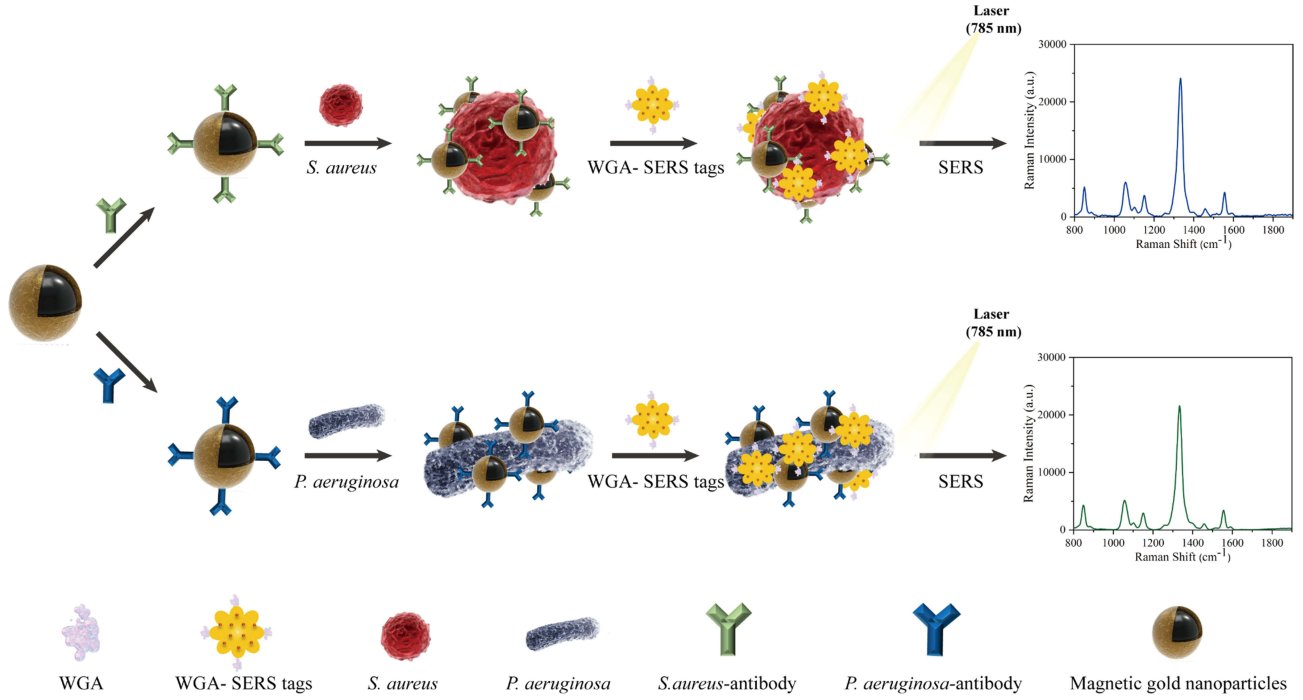

Several promising biosensors based on fluorescence, chemiluminescence, electrochemistry, and surface plasmon resonance have been developed to address challenges in clinical microbial testing.[7,8] Among these methods, label-based surface-enhanced Raman scattering (SERS) stands out as a potent analytical technique extensively applied in bacterial detection.[9–11] SERS tags, at the core of SERS biosensors, are nanoprobes with SERS activity, capable of recognizing the target and generating a significant and specific Raman signal.[12] Typical SERS tags include biorecognition elements for identifying target bacteria, precious metal nanomaterials, and specific Raman reporter molecules.[13] For instance, Zhu et al modified aptamer and 4-aminothiophenol (4-ATP) on gated aminated mesoporous silica nanoparticles (MSNs) as a SERS substrate for detecting *Staphylococcus aureus (S. aureus)*.[14] Zhuang et al designed ultra-sensitive SERS tags using gold nanostars (AuNSs) and 4-mercaptobenzoic acid (4-MBA) for detecting *Salmonella typhimurium (S. typhimurium)* in milk and meat samples.[15]

Currently, the development of such methods faces a critical and complex challenge concerning the preparation of SERS tags, requiring good stability, substantial Raman signal enhancement, and efficient binding to target bacteria. However, conventional colloidal gold and colloidal silver nanoparticles exhibit limited signal amplification. Additionally, the production of multifunctional nanoparticles is both time-consuming and challenging.[16] In the construction of dual-recognition SERS biosensors, it is often necessary to employ a pair of biorecognition molecules for identifying the target bacteria. Antibodies,[17] aptamers,[18] antibiotics[19] (eg, vancomycin), and antimicrobial peptides[20] are among the most widely used biorecognition agents. Antibodies, especially monoclonal antibodies, are highly homogeneous and recognize only a specific antigenic epitope. The high affinity allows antibodies to have higher detection sensitivity and binding ability to low concentrations of target molecules, making them one of the most commonly used types of antibodies in current in vitro diagnostic studies. However, antibodies are produced through animal immunization and can incur high costs when employed in assay labels requiring a large number of recognition elements.[21] Furthermore, aptamers require additional time and specific ions to unfold their spatial structure, posing challenges in screening for aptamers with high binding affinity to the target bacteria.[22] Consequently, the scarcity of dependable bacterial identification elements restricts the widespread application of label-based SERS detection.

In recent research, lectins have emerged as promising agents for pathogen capture, given their favorable characteristics such as low cost, high stability, and widespread availability.[23] Wheat germ agglutinin (WGA), one of the most researched and least immunogenic lectins, binds explicitly to N-acetyl-D-glucosamine and N-acetyl-D-glucosamine derivatives on bacterial surfaces.[24,25] Considering the prevalence of polysaccharides on bacterial surfaces, WGA exhibits immense potential for diverse applications in bacterial detection.[26] For example, Yang et al successfully and affordably identified *S. aureus* in blood samples by modifying WGA on magnetic gold nanoparticles (MGNPs) and combining it with a colorimetric method.[27] Tu et al employed WGA-modified magnetic quantum dots as a versatile assay nanoprobe to create a highly sensitive, multiplexed lateral flow assay for detecting *Pseudomonas aeruginosa (P. aeruginosa)* and *S. typhimurium* in complex samples.[28]

To enhance the detection sensitivity of SERS biosensors, a novel dual-recognition SERS biosensor was designed by incorporating WGA with high-performance AuNSs. Model bacteria, including Gram-positive *S. aureus* and Gram-negative *P. aeruginosa*, were selected to assess the universal detection capability of the platform. The developed approach involves three key steps. Firstly, target bacteria were captured by MGNPs modified with antibodies. Subsequently, WGA-SERS tags were introduced into the solution to form a sandwich structure (MGNPs/bacteria/SERS tags). The resulting SERS signal from this sandwich structure was promptly analyzed using Raman spectroscopy. Furthermore, the platform demonstrates versatility in detecting various pathogenic bacteria, allowing the easy replacement of specific antibodies tailored to different bacterial strains. We anticipate that this method will provide valuable insights into universal testing for the diagnosis of clinical bacterial infections.

Materials and Methods

Materials

5.5'-dithiobis-(2-nitrobenzoic acid) (DTNB), Bovine serum albumin (BSA), Polyethylenimine (PEI, MW ~25 kDa), Polyvinylpyrrolidone (PVP, MW 40 K), N-(3-dimethylaminopropyl)-N'-ethylcarbodiimide (EDC), N-hydroxysulfosuccinimide (sulfo-NHS), 2-(N-morpholino) ethanesulfonic acid (MES), phosphate buffered saline (PBS), Tween-20, and Wheat germ agglutinin lectin from Triticum vulgaris (WGA) were obtained from Sigma-Aldrich (St. Louis, MO, USA). Chloroauric acid tetrahydrate ($HAuCl_4 \cdot 4H_2O$), sodium borohydride ($NaBH_4$), 1×Phosphate-buffered saline (PBS, pH 7.4), ethanolamine hydroxylamine hydrochloride, hydroquinone, sodium dodecyl sulfate (SDS) and trisodium citrate (TSC) were obtained from Sinopharm Chemical Reagent Co (Shanghai, China). Mouse monoclonal anti-*S. aureus* antibodies (Catalog no. ab20920) and mouse monoclonal anti-*P. aeruginosa* antibodies (catalog no. ab68538) were brought from Abcam (Cambridge, United Kingdom).

The UV−vis absorption spectra were recorded using the Shimadzu 2600 spectrometer. Transmission electron microscope (TEM) images of nanocomposites were acquired with a Hitachi H-7650 microscope operating at 80 kV. Scanning electron microscopy (SEM) (JTOL JSM-7001 F) was employed to capture the surface morphology. Raman measurements were performed using a B&W Tek portable Raman spectrometer (i-Raman Plus BWS465-785H) with a 785 nm excitation laser. All Raman spectra were integrated for 10s with 10 mW power.

Acquisition of Bacterial Samples

The standard bacterial strains used in this study, including *S. aureus* ATCC 25923, *P. aeruginosa* ATCC 27853, and *Escherichia coli* (*E. coli*) ATCC 43888, were purchased from Solarbio Life Science (Beijing, China). *Listeria monocytogenes* (*L. monocytogenes), Klebsiella pneumoniae* (*K. pneumoniae*), and *Acinetobacter baumannii* (*A. baumannii*) were provided by the Xiao team from the Beijing Institute of Radiation Medicine.[29] Bacterial concentrations were verified using the classical plate count method.[30,31] In brief, *S. aureus* and *P. aeruginosa* were incubated on 5% sheep blood agar plates for 12 hours. A few colonies were picked from the plate and dispersed in PBS buffer (pH 7.4, 10 mM) to prepare a bacterial suspension. The initial bacterial solution was diluted in sterile water 1×10^5 to 10^6 times, and 100 μL of this dilution was coated on the blood agar plate at 37 °C. Colony-forming

units (CFU) on the plate were counted after 12 hours of incubation, and the final bacterial solution was further diluted to obtain various experimental concentrations.

MGNPs Assembly

The synthesis pathway of antibody - modified MGNPs is illustrated in Figure 1A. Monodispersed MGNPs were synthesized using the method described in our earlier publication.[32–34] Briefly, we opted for Fe_3O_4 magnetic nanoparticles (MNPs) as the superparamagnetic core to produce MGNPs, leveraging its robust magnetic responsiveness and stability. The synthesis involved the sequential self-assembly of a positively charged polyethyleneimine (PEI) layer and negatively charged 3 nm Au NPs on the MNPs surface to form MNPs-Au seed MNPs. Ultimately, through the in situ reduction of Au^{3+} on the compact 3 nm Au seed, we achieved the swift formation of uniform Au nanoshells with notable roughness, resulting in multifunctional MGNPs. Second, 20 mM MUA ethanol solution was added under sonication for 20 min for surface carboxylation. Then, the formed MGNPs were resuspended in 1 mL of MES solution (0.1 M, pH 6.0) containing 5 mM EDC under sonication. Third, antibody-modified MGNPs were accomplished through the COOH–NH2 condensation reaction of MUA and antibody. After the reaction for 2 h, 100 μL of BSA solution (10%) was added for an additional 1 h to block superfluous residual carboxyl. Finally, antibody-modified MGNPs were isolated using a magnet, and the isolated particles were rinsed once with PBS before being dispersed in 1 mL of PBS.

Preparation of WGA-SERS Tags

High-performance AuNSs were synthesized via a seed-mediated growth approach, as illustrated in Figure 2A. First, ~20 nm gold seeds were prepared using a modified Turkevich method. Briefly, 50 μL of $HAuCl_4$ (1%, w/v) and 150 μL of TSC (1%, w/v) were mixed in 5 mL boiling deionized water, stirred for 15 min, and placed at room temperature to cool down. Second, 150 μL of seed solution was mixed with 100 μL of 1% $HAuCl_4$ and 10 mL of deionized water under vigorous stirring. Then,

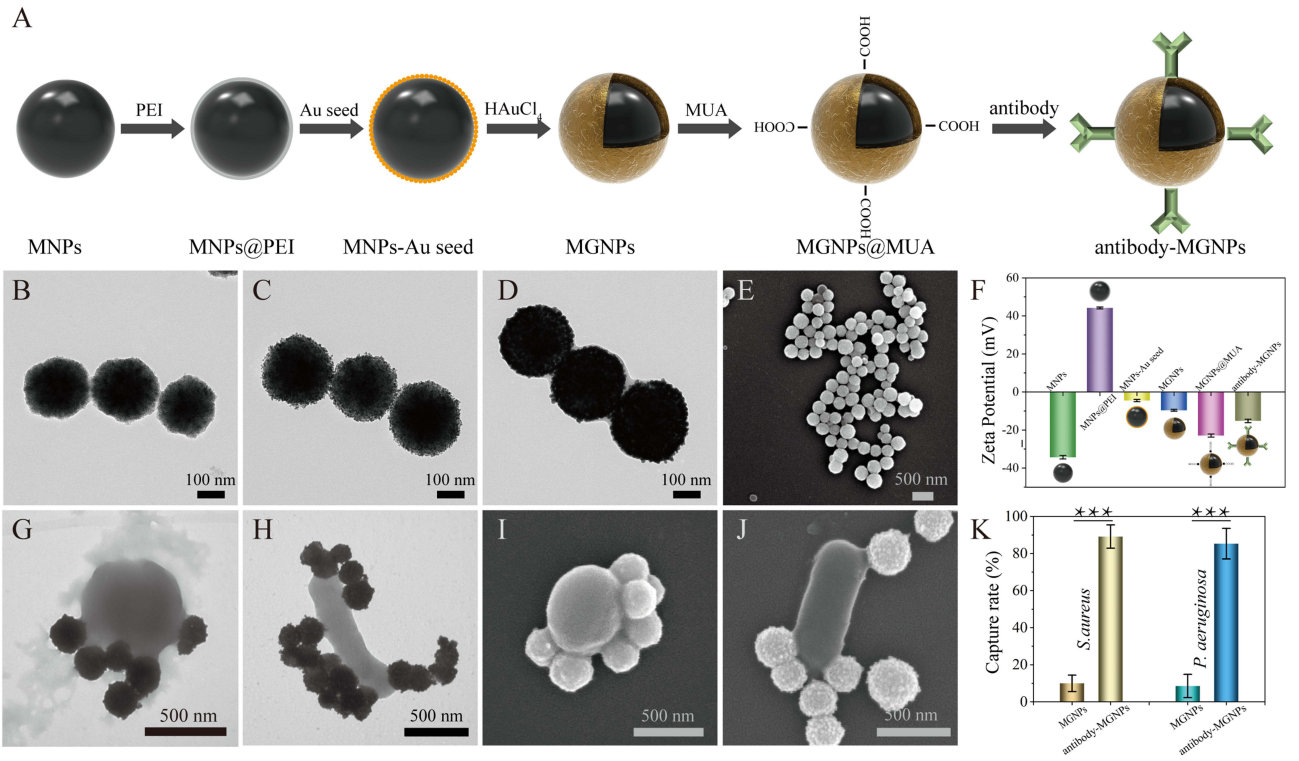

Figure 1 Characterization of the synthesized antibody-modified MGNPs. (**A**) Schematic diagram of the synthesis process of antibody-MGNPs. TEM images of (**B**) MNPs, (**C**) MNPs-Au seed, and (**D**) MGNPs. (**E**) SEM image of MGNPs. (**F**) Zeta potentials of the antibody-MGNPs from each stage. (**G-J**) TEM and SEM images of *S. aureus* and *P. aeruginosa* captured by antibody-MGNPs. TEM images of *S. aureus* (**G**) and *P. aeruginosa* (**H**) with antibody-MGNPs. SEM images of *S. aureus* (**I**) and *P. aeruginosa* (**J**) with antibody-MGNPs. (**K**) Capture efficiency of non-modified MGNPs and antibody-MGNPs. ***$p < 0.001$.

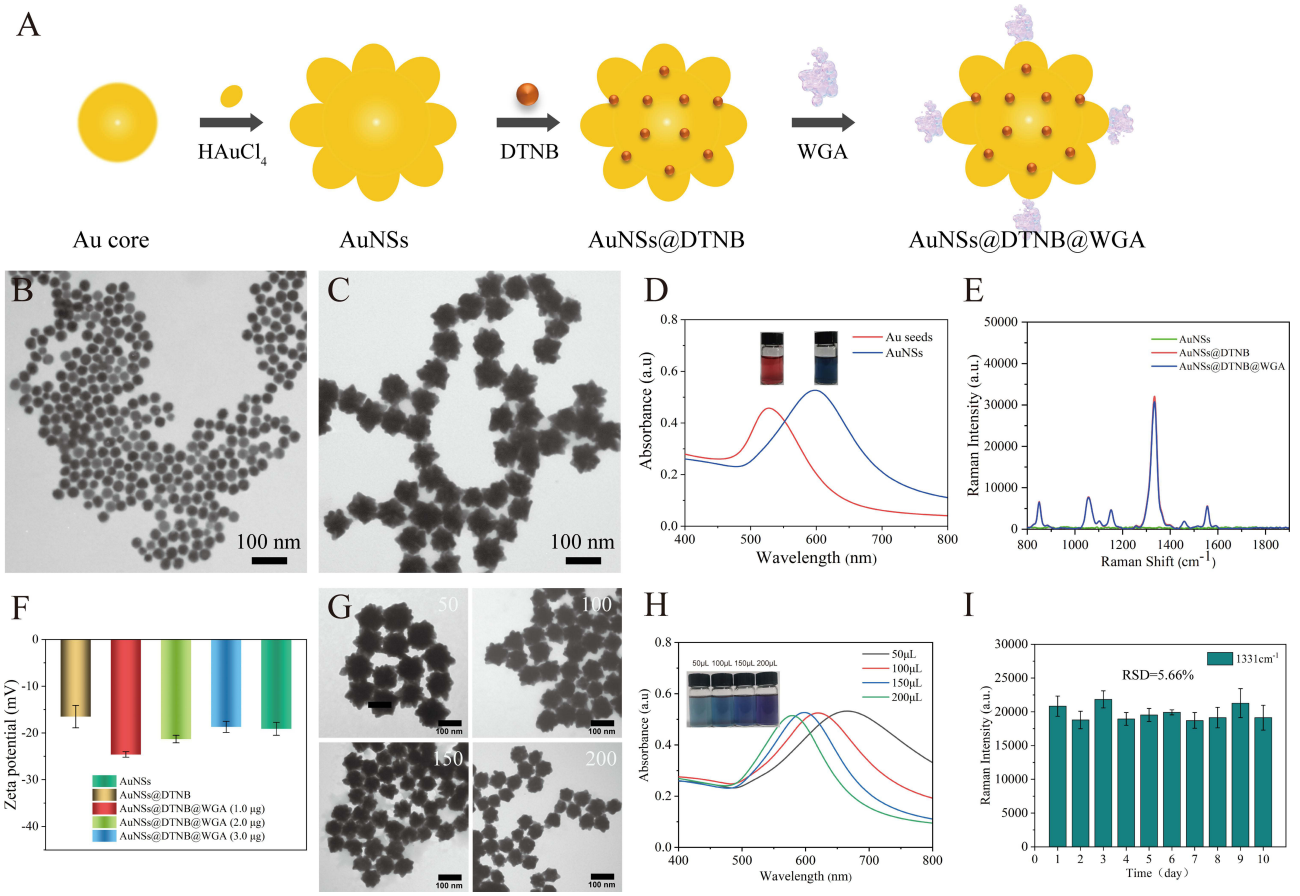

Figure 2 Characterization and optimization of the synthesized WGA-SERS tags. (**A**) Schematic diagram of the synthesis process of WGA modified AuNSs@DTNB. TEM images of (**B**) Au core, and (**C**) AuNSs. (**D**) UV-vis spectra of Au core (red) and AuNSs (blue). (**E**) SERS intensities of AuNSs, AuNSs@DTNB and AuNSs@DTNB@WGA. (**F**) Zeta potentials in each synthesis stage of WGA-SERS tags. (**G**) TEM images of AuNSs prepared with different seed amounts. (**H**) UV-vis spectra of AuNSs prepared with different seed amounts. (**I**) Raman intensities of the WGA-SERS tags against preservation time.

200 μL of 1% SDS, 50 μL of 1% TSC, and 500 μL of 60 mM hydroquinone were introduced into the solution simultaneously. Finally, the mixture was stirred at room temperature for 20 min to obtain an apparent blue-colored solution.

The WGA-conjugated SERS tags (WGA-SERS tags) were functionalized with AuNSs by using carbodiimide chemistry. In brief, 100 μL of 10^{-2} M Raman reporters DTNB in ethanol was mixed with 100 mL of AuNSs solution and stirred overnight at room temperature. Then, the prepared AuNSs@DTNB (2 mL) were separated by centrifugation (4500 rpm, 6 min) and then re-suspended in 1 mL of MES buffer (10 mM, pH 5.5). To link the DTNB through amide condensation, for this 5 μL of EDC (10 mM) and 10 μL of NHS (10 mM) were mixed followed by the addition of 2.0 μg WGA for 15 min. At the end of 2 h incubation step, 50 μL of BSA (10%) was added to the mixture and agitated for an additional hour to block unreacted carboxyl groups. The mixture was then isolated by centrifugation at 4500 rpm for 6 min to remove the supernatant. The precipitate was then redispersed in PBS (2 mM, pH 7.4) and labeled as WGA-SERS tags.

Bacteria Detection via SERS Strategy

In a typical experiment, 2 μL of antibody-modified MGNPs (10 mg/mL) and 1 mL of *S. aureus* or *P. aeruginosa* solutions within a range of 10–10^6 CFU/mL were mixed and incubated at 37 °C for 15 min. The non-captured bacteria were removed by magnetic separation and PBS washing twice, and the formed MGNPs/bacteria complexes were suspended in 100 μL of binding buffer (10 mM PBS, 5 mM Ca^{2+}, 5 mM Mg^{2+}). Afterward, the 60 μL of WGA-SERS tags were directly incubated with the above solutions for 15 min on an oscillator at room temperature. Finally, the formed MGNPs/bacteria/SERS tag sandwich complexes were magnetically collected, washed twice with PBS under a magnetic field, and transferred onto a Si chip for subsequent SERS detection using portable Raman spectrometer.

Analysis of Actual Samples

Human urine served as the authentic biological sample. A recovery experiment was performed to enhance the method's reliability. Samples were promptly collected from three healthy volunteers in our laboratory immediately after voiding. Informed consent was obtained from all volunteers participating in this study, and the study protocol adhered to the principles outlined in the Declaration of Helsinki. The study received approval from the research ethics committee of Guangdong Provincial People's Hospital (KY-X-2022-003-03).

Various concentrations of *S. aureus* or *P. aeruginosa* (5000, 500, 50 CFU/mL) were intentionally introduced into pooled urine samples from healthy volunteers to simulate real-world conditions. Subsequently, 2 μL of antibody-MGNPs were added, and the mixture was oscillated using an oscillator for 15 min. After magnetic separation, 60 μL of WGA-SERS tags were added to form a stable sandwich composite structure. The resulting complexes were analyzed using a portable Raman spectrometer, with each test being repeated three times.

Statistical Analysis

Each experiment was replicated at least three times, and the data were presented as mean ± SD. Statistical analysis employed One-Way ANOVA to assess differences, with significance denoted by $p < 0.05$.

Results and Discussion

Sensitive detection of *S. aureus* or *P. aeruginosa* relies on MGNPs modified with antibodies, serving as capture probes, and AuNSs immobilized with DTNB and WGA, functioning as signal probes. The operational procedure of the dual-recognition SERS biosensor involves three key steps, as illustrated in Scheme 1. First, MGNPs labeled with specific antibodies for either *S. aureus* or *P. aeruginosa* are mixed with a sample containing one or more bacterial species. The mixture is then incubated for 15 min, facilitating the specific binding of antibodies to the target bacteria. As specific pathogen recognition probes, MGNPs rely on the specificity of antibodies to concentrate and isolate bacteria using magnetic fields, especially when dealing with complex samples containing multiple bacterial species. Next, the proposed SERS tags are added and incubated for an additional 15 min to form sandwich structures. The AuNSs, modified with WGA as a strong affinity recognition molecule, bind to the peptidoglycan of the bacterial cell wall through strong hydrogen bonding. Finally, the sandwich complexes are collected using an external magnet, rinsed twice with PBST solution, and analyzed for SERS signals using a Raman instrument. Quantitative detection is performed based on the correlation between the characteristic signal intensity of DTNB carried by the sandwich structure and bacterial concentration. Importantly, utilizing high-performance tags and magnetic enrichment leads to a dual enhancement of SERS signals from target bacteria, significantly improving the sensitivity of SERS platforms based on sandwich analysis.

As previously reported, monodisperse MGNPs were synthesized as magnetic separators and SERS substrates using a PEI-mediated seed growth technique. The process of MGNPs synthesis is illustrated in Figure 1A and has been validated through TEM and zeta potential measurements. In Figure 1B, 200 nm superparamagnetic MNPs were initially prepared using the classical solvothermal method. Hydrophilic PEI rapidly self-assembled on the surface of MNPs, forming a charged thin layer that efficiently adsorbed 3 nm gold seeds through electrostatic adsorption (Figure 1C). Subsequently, following the reduction of Au^{3+} on the surface of the 3 nm gold seeds, a 25 nm layer of gold shells formed on the surface of the MNPs, resulting in the formation of MGNPs (Figure 1D). Additional synthesized MGNPs were visualized in the SEM image (Figure 1E). The MUA molecule, serving as a linker on the surface of MGNPs, binds with antibodies through carbodiimide chemistry. As shown in Figure 1F, the zeta potential of MGNPs modified by MUA decreased from −9.6 mV to −22.9 mV, and dropped back to −15.2 mV after coupling with the antibody, thus indicating the successful binding of the antibody to MGNPs. Subsequent studies explored the effectiveness of this antibody-based magnetic separation system in capturing the target bacteria. After 15 min of incubation with 2 μL of MGNPs and 1000 CFU/mL of *S. aureus* and *P. aeruginosa* solutions, the solutions were magnetically separated using an external magnet. The supernatant solution was incubated on blood agar overnight to calculate the capture efficiency, while the binding of bacteria and MGNPs complexes was observed by TEM and SEM. As shown in Figure 1G-J, MGNPs were tightly bound to *S. aureus* and *P. aeruginosa* in the solution. After magnetic separation, colony counting of the supernatant showed

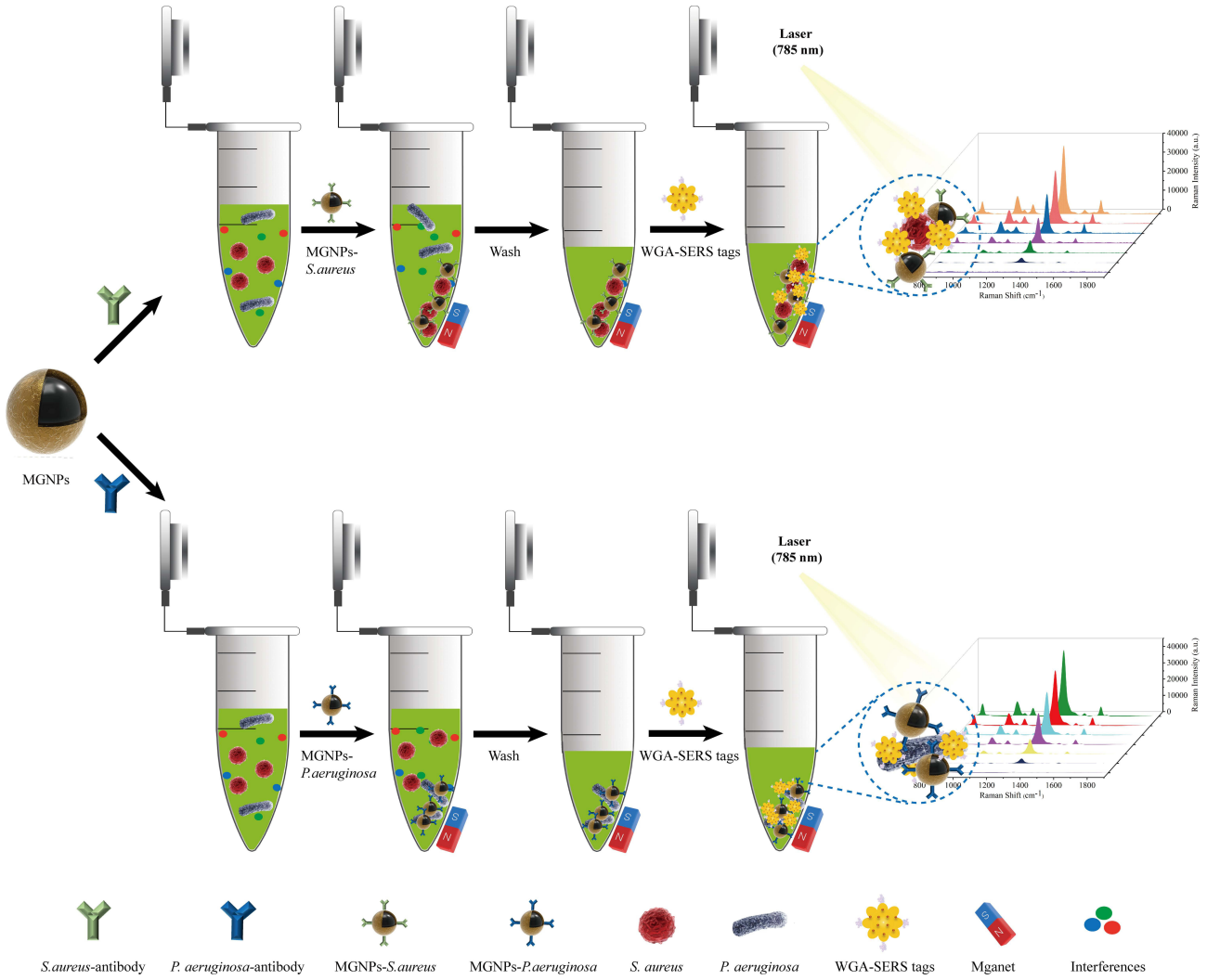

Scheme 1 Schematic illustration of the operating procedure for rapid detection of bacteria by using antibody-modified MGNPs and WGA-SERS tags in combination.

capture efficiencies of 89.13% and 85.31% for antibody-modified MGNPs against *S. aureus* and *P. aeruginosa*, respectively (Figure 1K), facilitating efficient isolation and enrichment of the target bacteria.

The WGA-SERS tags (AuNSs@DTNB@WGA) were synthesized using a seed-mediated growth strategy, as illustrated in Figure 2A. Initially, Au cores with an average size of 20 nm were synthesized through the sodium citrate reduction method (Figure 2B). Subsequently, TSC and hydroquinone acted as reducing and capping agents on the surface of the Au cores, converting Au^{3+} to Au^{0} and enabling the Au cores to grow into star-shaped gold nanostructures with multiple technical angles. The TEM image (Figure 2C) revealed nanoscale raised tips on the surface of each AuNS, significantly enhancing the potential "hot spots" in the local field. The formation of star-shaped gold nanostructures caused a shift in the absorption band of the burgundy Au cores in the UV-Vis spectrum from 526 nm to 596 nm, and the solution color turned dark blue (Figure 2D). DTNB molecules covering the surface of AuNSs provided characteristic SERS signals and carried carboxyl groups that could be conjugated to WGA. The SERS spectra of AuNSs, AuNSs@DTNB, and AuNSs@DTNB@WGA (WGA-SERS tags) were measured and analyzed, as shown in Figure 2E. After WGA modification, almost no discernible spectral differences were observed for AuNSs@DTNB, confirming the Raman detection capability of the WGA-modified SERS tags. Successful verification of WGA conjugation with AuNSs was achieved through zeta potential monitoring. The zeta potential of unmodified AuNSs in Figure 2F was −16.5 mV, which decreased further to −23.6 mV after DTNB modification. Subsequently, the zeta potential slightly increased after WGA conjugation, stabilizing at −18.7 mV upon saturation with WGA (exceeding 2 μg), indicating sufficient binding of 2 μg WGA and AuNSs@DTNB.

Controlled volumes of seed solution (50, 100, 150, and 200 μL) were systematically used to synthesize a variety of AuNSs with different sizes. As the volume of the seed solution increased, there were notable alterations in the structure and size of the resulting AuNSs, as illustrated in Figure 2G. The diameter of the AuNSs decreased from 120 nm to 50 nm, accompanied by a gradual blue-shift in the LSPR peak and a transition in solution color from blue to purple (Figure 2H). AuNSs featuring a diameter of 65 nm were selected for subsequent experiments, considering the spatial site resistance effect of SERS tags. Furthermore, the WGA-SERS tags, prepared using these AuNSs, exhibited negligible changes in SERS signals even after storage at 4 °C for 10 days (Figure 2I). The relative standard deviation (RSD) of the Raman signal intensity at 1331 cm^{-1} was measured at 5.66%, underscoring the commendable storage stability of the freshly prepared WGA-SERS tags.

The practical application of the sensor heavily relies on the effectiveness of the synthesized SERS tags in binding to pathogenic bacteria. In previous studies, we demonstrated that WGA-modified MGNPs exhibited a strong affinity for binding to various pathogenic bacteria, including *S. epidermidis, P. aeruginosa, S. aureus, L. mono, E. coli, A. baumannii, S. sonnei*, and *S. typhi*.[35,36] In this study, we investigated the binding capability of SERS tags, which were modified with varying levels of WGA, to interact with pathogenic bacteria. The *S. aureus* model was used as our experimental example. The dynamic process of binding was confirmed through TEM image observation and SERS signal detection using a portable Raman spectrometer (Figure 3A and B). With an increase in WGA modification from 0.25 μg to 2.5 μg, the number of SERS tags bound to the bacterial surface gradually increased. Notably, at a WGA modification of 2.0 μg, the WGA-SERS tags adhered densely and uniformly to the bacterial surface, as depicted in Figure 3A. Importantly, the statistical analysis revealed no significant difference in signal values (Figure 3B, $p > 0.05$). In summary, the synthesized SERS tags, especially those modified with 2.0 μg of WGA, demonstrated robust binding capabilities, as evidenced by the attachment of the tags to the bacterial surfaces.

In this study, we conducted a comprehensive comparative analysis of SERS tags using conventional AuNPs and our proposed AuNSs as enhanced substrates for the detection of target bacteria, employing an equivalent concentration of WGA. TEM images presented in Figure 3C and D demonstrate that within the MGNPs/bacteria/SERS tags complexes, a higher number of AuNSs adhered to *S. aureus* and *P. aeruginosa* compared to AuNPs. This observation is attributed to the heightened SERS-enhancing capability and surface extensibility of AuNSs. Specifically, the SERS tags utilizing AuNSs as the enhancement substrate exhibited a significant increase in Raman signals on the surfaces of MGNPs-enriched bacteria, as shown in Figure 3E and F ($p < 0.05$). These findings emphasize the superior performance of SERS tags incorporating AuNSs@WGA in bacterial detection.

To assess the detection capability of the developed assay, bacterial samples of *S. aureus* and *P. aeruginosa* spanning a concentration range of $10–10^6$ CFU/mL were meticulously prepared through gradient dilution. The implementation of the dual-identification SERS detection platform followed the proposed procedure, involving the separate incubation of MGNPs and bacteria, addition of equal amounts of WGA-SERS tags to form a sandwich structure, and the subsequent measurement of the Raman intensity at 1331 cm^{-1} of DTNB. As illustrated in Figure 4A and B, the results for different concentrations of *S. aureus* and *P. aeruginosa* reveal a gradual increase in the intensity of the SERS signal with the rising concentration of bacteria in the sample. Calibration curves, depicted in Figure 4C and D, were plotted by measuring the SERS signal intensity against the bacterial concentration of the two target bacteria. The SERS signal at Raman shift 1331 cm^{-1} exhibited a linear correlation with *S. aureus* and *P. aeruginosa* in the range of $10–10^6$ CFU/mL ($R^2 = 0.987$ and 0.985), respectively. Calculating the limit of detection (LOD) using the 3-fold standard deviation of the blank control determined the LOD for our SERS assay platform for *S. aureus* and *P. aeruginosa* to be 7 and 5 CFU/mL, respectively. The novel WGA-SERS tags, benefiting from the remarkable Raman enhancement effect of AuNSs and the efficient binding of WGA to pathogenic bacteria, offered stable and strong Raman signals. WGA, as a versatile bacterial recognition element, not only ensures strong bacterial binding affinity but also does so at a relatively low cost. In comparison to our previous work involving gold nanorods (AuNRs),[37] two-dimensional molybdenum disulfide (MoS_2) nanosheets,[38] and graphene oxide (GO),[39] the proposed utilization of AuNSs as a novel SERS enhancement substrate introduces a simpler synthetic process and achieves superior SERS enhancement effects, enabling lower detection limits for the target bacteria. This strategic selection of SERS enhancement materials not only contributes to enhancing the stability and sensitivity of SERS tags but also broadens the potential application scope of bacterial detection.

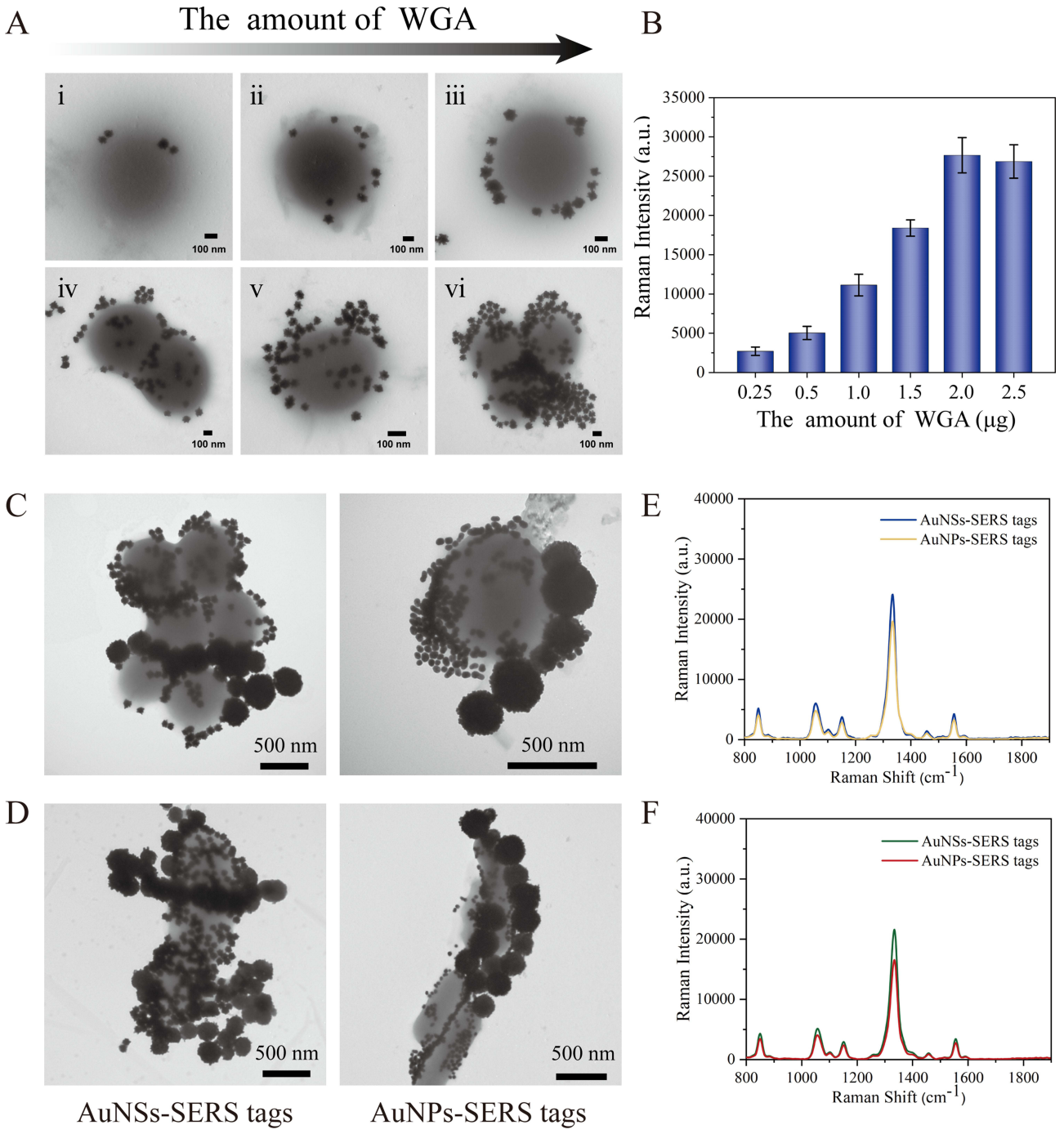

Figure 3 Comparative optimization of WGA-SERS tags. (**A**) TEM images of *S. aureus* bound to WGA-SERS tags with various amounts of WGA. i~iv represent WGA concentrations of 0.25~2.5 μg. (**B**) The corresponding SERS intensities of SERS tags with *S. aureus* in various amounts of WGA. TEM images of sandwich composite structures formed by AuNSs or AuNPs-SERS tags with MGNPs adsorbed on *S. aureus* (**C**) and *P. aeruginosa* (**D**). Corresponding SERS signal measured from sandwich composite structures formed by AuNSs or AuNPs-SERS tags with *S. aureus* (**E**) and *P. aeruginosa* (**F**).

Selectivity is a critical factor in determining the effectiveness of biosensors for practical applications. In this study, 10^5 CFU/mL of *S. aureus* or *P. aeruginosa* and other interfering strains (including *L. mono, K. pneumoniae, A. baumannii and E. coli*) were detected using our dual recognition SERS assay to evaluate the specificity of the developed platform. Figure 5A and B show the corresponding SERS spectra at 1331 cm^{-1} that could be detected only in the presence of *S. aureus* or *P. aeruginosa*, while the SERS signal for the non-target bacteria was very weak. To investigate the utility and reliability of our proposed SERS assay platform in biological samples, the method's recovery was evaluated by adding

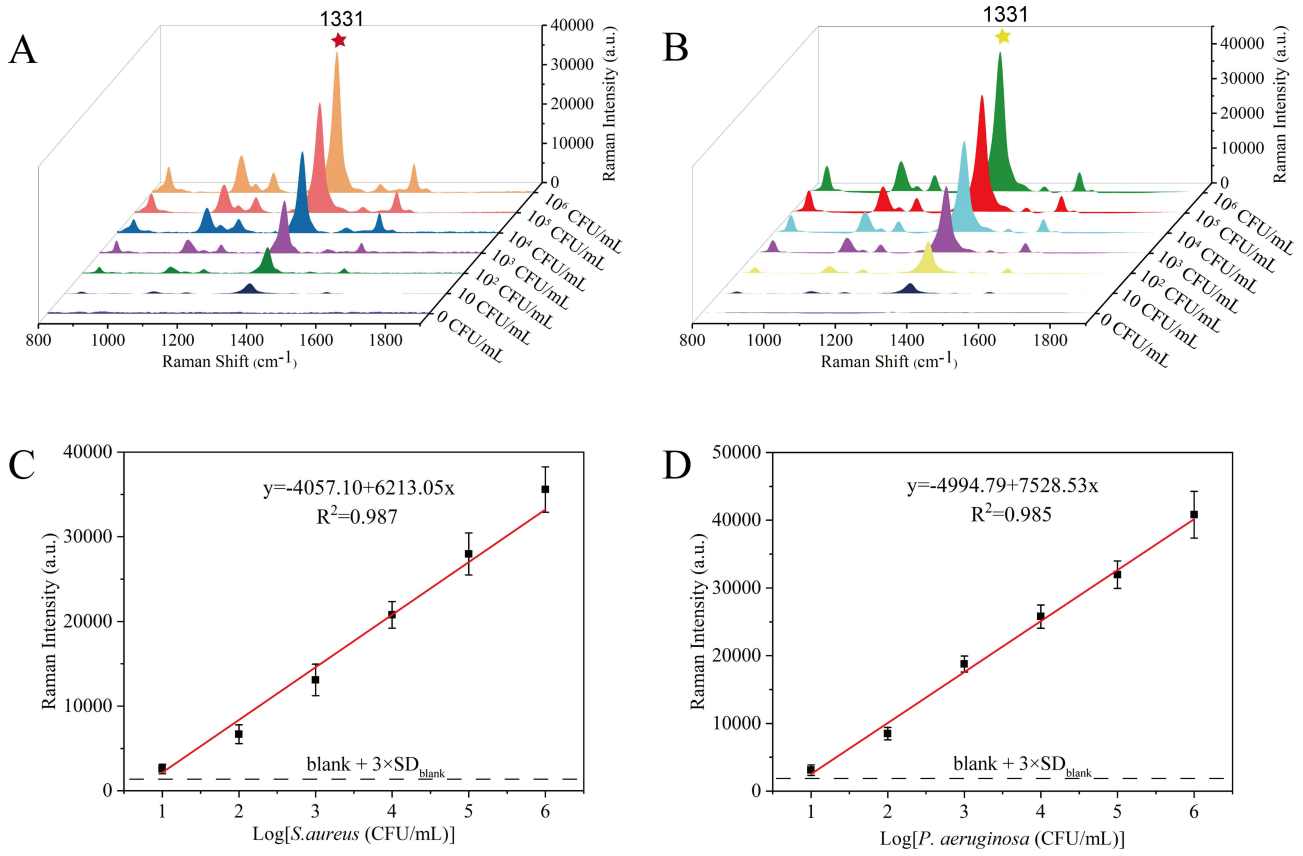

Figure 4 Evaluation of the quantitative detection ability of the SERS biosensor. The recorded SERS spectra for sandwich complexes formed with *S. aureus* (**A**) and *P. aeruginosa* (**B**) in the concentration range of 10–10^6 CFU/mL. Corresponding calibration curves of the proposed SERS platform for *S. aureus* (**C**) and *P. aeruginosa* (**D**). Each spectrum is the average of three independently collected spectra.

different concentrations of *S. aureus* and *P. aeruginosa* (5000, 500, 50 CFU/mL) to human urine samples. Figure 5C and D show that very clear and stable SERS signals were generated for all urine samples spiked with *S. aureus* or *P. aeruginosa*. The recoveries ranged from 84.8% to 118.0%, with RSD below 11.42% (Table 1), showcasing the high reliability of the method in detecting biological samples. Therefore, our proposed biosensor demonstrates excellent applicability and accuracy for detecting *S. aureus* and *P. aeruginosa*.

Conclusion

In conclusion, our study introduces a robust sandwich-structured SERS biosensor designed for the rapid and sensitive detection of *S. aureus* or *P. aeruginosa*. The incorporation of WGA-SERS tags, featuring WGA and DTNB-modified AuNSs, ensures strong anchoring to bacterial surfaces, facilitating stable Raman signal enhancement. Overcoming challenges associated with alternative recognition molecules, such as aptamers or antimicrobial peptides, our biosensor employs MNPs modified with specific antibodies as capture probes. The integration of magnetic separation of antibodies and the application of novel SERS tags significantly enhance the biosensor's detection capability, achieving sensitivities as low as 7 CFU/mL for *S. aureus* and 5 CFU/mL for *P. aeruginosa*. With high speed, reproducibility, and specificity, our biosensor is well-suited for efficiently detecting bacteria in human urine samples. To the best of our knowledge, this work is the first to propose the combination of WGA and SERS tags for fabricating high-performance SERS tags in bacterial detection. By replacing the recognition element of the capture probe, the proposed universal SERS biosensor holds the potential for detecting various other pathogenic bacteria. Our biosensor stands out as a promising tool in pathogen detection and bioanalytical research, presenting a valuable contribution to the field. Moving forward, future research could explore further optimization and extension of this innovative SERS biosensor technology in different application scenarios. To achieve this, extending the detection range of this biosensor to target more pathogens for rapid and sensitive

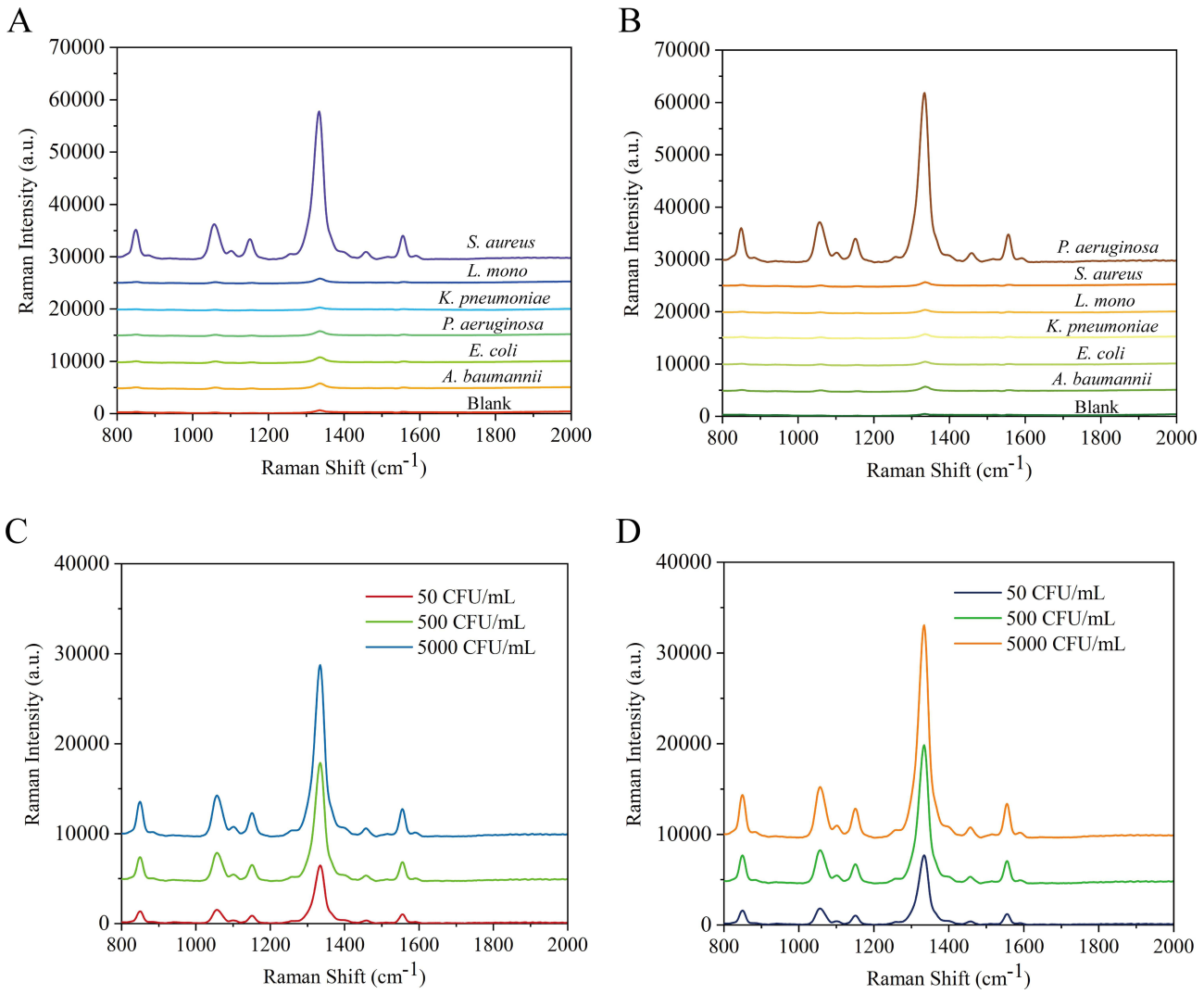

Figure 5 Comparison of the SERS spectra of interfering strains and *S. aureus* (**A**) and *P. aeruginosa* (**B**) detected by dual recognition SERS biosensors. The SERS spectra of *S. aureus* (**C**) and *P. aeruginosa* (**D**) in actual human urine samples were detected by dual recognition SERS biosensors.

detection is a promising avenue. Additionally, considering further integration of intelligent technologies could enhance the operability and convenience of the biosensor in real-world scenarios, paving the way for more practical applications in various fields.

Table 1 The Recovery Efficiency of *S. aureus* or *P. aeruginosa* in Human Urine Samples Using the Developed SERS Method

Strain	Concentration of Bacteria (CFU/mL)		Raman Intensity	Recovery (%)	RSD (%)
	Added	Detected			
S. aureus	5000	4651	18,723.92	93.0	9.58
	500	533	12,832.77	106.6	6.36
	50	59	6460.27	118.0	11.42
P. aeruginosa	5000	5220	22,987.81	104.4	6.96
	500	424	14,708.48	84.8	8.72
	50	57	7568.82	114.0	6.21

https://doi.org/10.2147/IJN.S433316 DovePress

Abbreviations

S. aureus, Staphylococcus aureus; P. aeruginosa, Pseudomonas aeruginosa; WGA, Wheat germ agglutinin; Abs, Antibodies; AuNSs, Gold nanostars, DTNB, 5.5'-dithiobis(2-nitrobenzoic acid); magnetic gold nanoparticles (MGNPs); LOD, limit of detection; SERS, Surface-enhanced Raman scattering.

Acknowledgments

We would like to express our sincere gratitude to Ping Yang, Nanjing Drum Tower Hospital, for his significant contributions to this research. Although not listed as a corresponding author, Ping Yang played a crucial role in data analysis and experimental design. His expertise and dedication greatly enriched the quality and depth of this study.

Funding

This research was supported by the National Natural Science Foundation of China (82072380, 82272423), Key R & D Program of Jiangsu Province (BE2020646), Research foundation for advanced talents of Guandong Provincial People's Hospital (KJ012021097), the Nanjing Drum Tower Hospital Clinical Research Special Fund project (2022-LCYJ-PY-36, 2022-LCYJ-MS-28).

Disclosure

The authors report no conflicts of interest in this work.

References

1. Atia AF, Afifi AF, Gaffer MMA, Elnahas NS, Oshiba SFA. Dendritic Cells as an Adjuvant to some Schistosoma mansoni Antigens for Vaccination in Experimental Schistosomiasis. *Int J Curr Microbiol Appl Sci*. 2020;9(3):32–53. doi:10.20546/ijcmas.2020.903.005
2. Molehin AJ. Schistosomiasis vaccine development: update on human clinical trials. *J Biomed Sci*. 2020;27(1):28. doi:10.1186/s12929-020-0621-y
3. Galvan DD, Yu Q. Surface-Enhanced Raman Scattering for Rapid Detection and Characterization of Antibiotic-Resistant Bacteria. *Adv Healthc Mater*. 2018;7(13):e1701335. doi:10.1002/adhm.201701335
4. Someko H, Okazaki Y, Tsujimoto Y, Ishikane M, Kubo K, Kakehashi T. Diagnostic accuracy of rapid antigen tests in cerebrospinal fluid for pneumococcal meningitis: a systematic review and meta-analysis. *Clin Microbiol Infect*. 2023;29:310–319. doi:10.1016/j.cmi.2022.12.002
5. Zhou Q, Natarajan B, Kannan P. Nanostructured biosensing platforms for the detection of food- and water-borne pathogenicEscherichia coli. *Anal Bioanal Chem*. 2023;415:3111–3129. doi:10.1007/s00216-023-04731-6
6. Hughes S, Troise O, Donaldson H, Mughal N, Moore LSP. Bacterial and fungal coinfection among hospitalized patients with COVID-19: a retrospective cohort study in a UK secondary-care setting. *Clin Microbiol Infect*. 2020;26(10):1395–1399. doi:10.1016/j.cmi.2020.06.025
7. Lindner F, Diepold A. Optogenetics in bacteria - applications and opportunities. *FEMS Microbiol Rev*. 2022;46:undefined. doi:10.1093/femsre/fuab055
8. Liu L, Zhang H, Xing S, et al. Copper-Zinc Bimetallic Single-Atom Catalysts with Localized Surface Plasmon Resonance-Enhanced Photothermal Effect and Catalytic Activity for Melanoma Treatment and Wound-Healing. *Adv Sci*. 2023;10(18):e2207342. doi:10.1002/advs.202207342
9. Dina N, Tahir M, Bajwa S, Amin I, Valev V, Zhang L. SERS-based antibiotic susceptibility testing: towards point-of-care clinical diagnosis. *Biosens Bioelectron*. 2022;219:114843. doi:10.1016/j.bios.2022.114843
10. Langer J, Jimenez de Aberasturi D, Aizpurua J, et al. Present and Future of Surface-Enhanced Raman Scattering. *ACS Nano*. 2020;14:28–117.
11. Huang X, Zhang Z, Chen L, et al. Multifunctional Au nano-bridged nanogap probes as ICP-MS/SERS dual-signal tags and signal amplifiers for bacteria discriminating, quantitative detecting and photothermal bactericidal activity. *Biosens Bioelectron*. 2022;212:114414. doi:10.1016/j.bios.2022.114414
12. Lane LA, Qian X, Nie S. SERS Nanoparticles in Medicine: from Label-Free Detection to Spectroscopic Tagging. *Chem Rev*. 2015;115(19):10489–10529. doi:10.1021/acs.chemrev.5b00265
13. Liu H, Gao X, Xu C, Liu D. SERS Tags for Biomedical Detection and Bioimaging. *Theranostics*. 2022;12(4):1870–1903. doi:10.7150/thno.66859
14. Zhu A, Jiao T, Ali S, Xu Y, Ouyang Q, Chen Q. SERS Sensors Based on Aptamer-Gated Mesoporous Silica Nanoparticles for Quantitative Detection of Staphylococcus aureus with Signal Molecular Release. *Anal Chem*. 2021;93(28):9788–9796. doi:10.1021/acs.analchem.1c01280
15. Zhuang J, Zhao Z, Lian K, et al. SERS-based CRISPR/Cas assay on microfluidic paper analytical devices for supersensitive detection of pathogenic bacteria in foods. *Biosens Bioelectron*. 2022;207:114167. doi:10.1016/j.bios.2022.114167
16. Wu Z, Zhou J, Nkanga C, et al. One-Step Supramolecular Multifunctional Coating on Plant Virus Nanoparticles for Bioimaging and Therapeutic Applications. *ACS Appl Mater Interfaces*. 2022;14(11):13692–13702. doi:10.1021/acsami.1c22690
17. Zhong Y, Zheng X, Li Q, Loh X, Su X, Zhao S. Antibody conjugated Au/Ir@Cu/Zn-MOF probe for bacterial lateral flow immunoassay and precise synergistic antibacterial treatment. *Biosens Bioelectron*. 2023;224:115033. doi:10.1016/j.bios.2022.115033
18. Xu Y, He P, Ahmad W, et al. Catalytic hairpin activated gold-magnetic/gold-core-silver-shell rapid self-assembly for ultrasensitive Staphylococcus aureus sensing via PDMS-based SERS platform. *Biosens Bioelectron*. 2022;209:114240. doi:10.1016/j.bios.2022.114240
19. Gao X, Yin Y, Wu H, et al. Integrated SERS Platform for Reliable Detection and Photothermal Elimination of Bacteria in Whole Blood Samples. *Anal Chem*. 2020;93(3):1569–1577. doi:10.1021/acs.analchem.0c03981
20. Cao H, Gao Y, Jia H, et al. Macrophage-Membrane-Camouflaged Nonviral Gene Vectors for the Treatment of Multidrug-Resistant Bacterial Sepsis. *Nano Lett*. 2022;22(19):7882–7891. doi:10.1021/acs.nanolett.2c02560

21. O'Neill E, Cosenza Z, Baar K, Block D. Considerations for the development of cost-effective cell culture media for cultivated meat production. *Compr Rev Food Sci Food Saf*. 2021;20(1):686–709. doi:10.1111/1541-4337.12678
22. Shin W, Ahn G, Lee J-P, et al. Recent Advances in Engineering Aptamer-based Sensing and Recovery of Heavy Metals and Rare Earth Elements for Environmental Sustainability. *Chem Eng J*. 2023;472:144742. doi:10.1016/j.cej.2023.144742
23. Mi F, Guan M, Hu C, Peng F, Sun S, Wang X. Application of lectin-based biosensor technology in the detection of foodborne pathogenic bacteria: a review. *Analyst*. 2021;146(2):429–443. doi:10.1039/D0AN01459A
24. Skoll K, Palmetzhofer J, Lummerstorfer M, Anzengruber M, Gabor F, Wirth M. Human serum albumin nanoparticles as a versatile vehicle for targeted delivery of antibiotics to combat bacterial infections. *Nanomedicine*. 2023;50:102685. doi:10.1016/j.nano.2023.102685
25. Masigol M, Fattahi N, Barua N, et al. Identification of Critical Surface Parameters Driving Lectin-Mediated Capture of Bacteria from Solution. *Biomacromolecules*. 2019;20(7):2852–2863. doi:10.1021/acs.biomac.9b00609
26. Grossman AS, Escobar CA, Mans EJ, et al. A Surface Exposed, Two-Domain Lipoprotein Cargo of a Type XI Secretion System Promotes Colonization of Host Intestinal Epithelia Expressing Glycans. *Front Microbiol*. 2022;13:800366. doi:10.3389/fmicb.2022.800366
27. Yang G, Meng X, Wang Y, Yan M, Aguilar ZP, Xua H. 2-Step lectin-magnetic separation (LMS) strategy combined with AuNPsbased colorimetric system for *S. aureus* detection in blood. *Sens Actuators B*. 2019;279:87–94. doi:10.1016/j.snb.2018.09.112
28. Tu Z, Yang X, Dong H, et al. Ultrasensitive Fluorescence Lateral Flow Assay for Simultaneous Detection of Pseudomonas aeruginosa and Salmonella typhimurium via Wheat Germ Agglutinin-Functionalized Magnetic Quantum Dot Nanoprobe. *Biosensors*. 2022;12(11):942. doi:10.3390/bios12110942
29. Zheng S, Yang X, Zhang B, et al. Sensitive detection of Escherichia coli O157:H7 and Salmonella typhimurium in food samples using two-channel fluorescence lateral flow assay with liquid Si@quantum dot. *Food Chem*. 2021;363:130400. doi:10.1016/j.foodchem.2021.130400
30. Li J, Wang C, Shi L, et al. Rapid identification and antibiotic susceptibility test of pathogens in blood based on magnetic separation and surface-enhanced Raman scattering. *Mikrochim Acta*. 2019;186(7):475. doi:10.1007/s00604-019-3571-x
31. Molina-Mora J, Fernando GG. Molecular Determinants of Antibiotic Resistance in the Costa Rican Pseudomonas aeruginosa AG1 by a Multi-omics Approach:A Review of 10 Years of Study. *Phenomics*. 2021;3:129–142. doi:10.1007/s43657-021-00016-z
32. Zhou Z, Xiao R, Cheng S, et al. A universal SERS-label immunoassay for pathogen bacteria detection based on Fe3O4@Au-aptamer separation and antibody-protein A orientation recognition. *Anal Chim Acta*. 2021;1160:338421. doi:10.1016/j.aca.2021.338421
33. Tu J, Wu T, Yu Q, et al. Introduction of multilayered magnetic core-dual shell SERS tags into lateral flow immunoassay: a highly stable and sensitive method for the simultaneous detection of multiple veterinary drugs in complex samples. *J Hazard Mater*. 2023;448:130912. doi:10.1016/j.jhazmat.2023.130912
34. Liu X, Yang X, Li K, et al. Fe3O4@Au SERS tags-based lateral flow assay for simultaneous detection of serum amyloid A and C-reactive protein in unprocessed blood sample. *Sens Actuators B*. 2020;320:128350. doi:10.1016/j.snb.2020.128350
35. Tu Z, Cheng S, Dong H, et al. Universal and ultrasensitive detection of foodborne bacteria on a lateral flow assay strip by using wheat germ agglutinin-modified magnetic SERS nanotags. *RSC Adv*. 2022;12(42):27344–27354. doi:10.1039/D2RA04735G
36. Cheng S, Tu Z, Zheng S, et al. An efficient SERS platform for the ultrasensitive detection of Staphylococcus aureus and Listeria monocytogenes via wheat germ agglutinin-modified magnetic SERS substrate and streptavidin/ aptamer co-functionalized SERS tags. *Anal Chim Acta*. 2021;1187:339155. doi:10.1016/j.aca.2021.339155
37. Wang J, Wu X, Wang C, et al. Facile synthesis of Au-coated magnetic nanoparticles and their application in bacteria detection via a SERS method. *ACS Appl Mater Interfaces*. 2016;8(31):19958–19967. doi:10.1021/acsami.6b07528
38. Yu Q, Li J, Zheng S, et al. Molybdenum disulfide-loaded multilayer AuNPs with colorimetric-SERS dual-signal enhancement activities for flexible immunochromatographic diagnosis of monkeypox virus. *J Hazard Mater*. 2023;459:132136. doi:10.1016/j.jhazmat.2023.132136
39. Wang C, Wang C, Li J, et al. Ultrasensitive and multiplex detection of four pathogenic bacteria on a bi-channel lateral flow immunoassay strip with three-dimensional membrane-like SERS nanostickers. *Biosens Bioelectron*. 2022;214:114525. doi:10.1016/j.bios.2022.114525